Electronic Supplementary Information For:

Manipulation of Peptide-Fatty Acid Bioconjugates on Graphene: Effects of Fatty Acid Chain Length and Attachment Point

Yuliana Perdomo,[a,#] *Ruitao Jin,* [b,#] *Atul D. Parab,*[a] *Marc R. Knecht* [a,c,‡,]* *and Tiffany R. Walsh* [b,‡,]*

[a]Department of Chemistry, University of Miami, 1301 Memorial Drive, Coral Gables, Florida 33146, United States,

[b]Institute for Frontier Materials, Deakin University, Geelong, Victoria 3216, Australia

[c]Dr. J.T. Macdonald Foundation Biomedical Nanotechnology Institute, University of Miami, UM Life Science Technology Building, 1951 NW 7th Ave, Suite 475, Miami, Florida, 33136, United States

([‡]: These authors contributed equally)

([#]: These authors contributed equally)

*To whom correspondence should be addressed: MRK: Phone: (305) 284-9351, email: knecht@miami.edu; TRW: Phone: +61 (35) 227-3116, email: tiffany.walsh@deakin.edu.au

Computational Methodology

System Setup:

Eight all-atom REST-MD simulations[1, 2] were performed using the Gromacs v 2021.1 software package,[3] one for each of the eight bioconjugate molecules. Each simulation system comprised one bio-conjugate molecule, one periodic graphene sheet, and liquid water (~18,000 water molecules). The graphene sheet was placed in an orthorhombic periodic simulation cell with dimensions 8.9nm x 8.9nm x 7.5nm, oriented in the *x*-*y* plane. The vertical inter-sheet gap between graphene and its periodic image (along the z-dimension) was filled with liquid water and counter-ions. All simulations were performed in the Canonical (*NVT*) ensemble at 300 K, using the Nose-Hoover thermostat.[4, 5] at a thermal temperature of 300K, with a coupling constant of τ=0.2 ps. Newton's equations of motion were solved with an integration time-step of 1fs. Coordinates were saved every 1ps. Long-ranged electrostatic interactions were treated using Particle-mesh Ewald (PME),[6] with a cut-off at 11 Å, whereas a force-switched cut-off ending at 10 Å was used for the Lennard-Jones non-bonded interactions. A previously-tested force-field combination was used comprising CHARMM22*[7, 8] for the peptides (with parameter modifications to describe the maleimide-mediated fatty acid linkage, as reported previously)[9] and the polarizable GRAPPA[10] force-field for graphene, along with the modified TIP3P[11, 12] force-field for water.Following previous work,[13, 14] all carbon atoms in the graphene sheet were held fixed in space during these simulations except those dipoles which were able to freely rotate.

REST-MD Simulation Details:

In these REST-MD simulations, 20 replicas were used with an 'effective temperature' range of 300-430 K. The initial structures of the 20 replicas were based on those used from a previous study of $P1CF_{10}$ and $F_{10}CP1$.[13] The REST-MD trajectories were of 20 ns duration (amounting to 20 × 20 ns = 0.4 μs of nominal total simulation time). The 20 values of lambda used to scale the force-field were: λ_i =0.0 0.0526 0.1053 0.1579 0.2105 0.2632 0.3158 0.3684 0.4211 0.4737 0.5263 0.5789 0.6316 0.6842 0.7368 0.7895 0.8421 0.8947 0.9474 and 1.000. The 20 initial configurations were energy minimized and then equilibrated at their target potential for 0.5 ns, with no exchange moves attempted during this period. During the replica exchange period, exchanges were attempted every 1 ps.

Simulation Analysis:

The degree of residue-surface contact was determined by calculating the fraction of the total REST-MD reference trajectory (*i.e.* the trajectory that corresponds to the unscaled Hamiltonian, λ=0.0) that a reference site on a residue was less than or equal to a cutoff distance of the graphene surface, calculated by using the perpendicular component of the distance only (in the z-direction). The reference sites and cutoff-distances (for graphene) were the same as those used in previous work[14] and are provided in Table S1 for convenience.

Table S1. Summary of cut-off distances and reference sites used to determine residue-surface contact.

Residue	Reference Site and Cutoff Distance (Å) on Graphene
Ala	CB, 5Å
Asp	CG, 5Å
Asn	ND2, 4.5Å
Cys	SG, 4.5Å
Gln	NE2, 4.5Å
His	Center of mass of ring, 4.5Å
Leu	CG, 5Å
Lys	NZ, 6Å
Phe	Center of mass of ring, 4Å
Ser	OG, 4.25Å
Thr	OG1, 4.25Å
Trp	Mid of central bond, 3.7Å
Tyr	Center of mass of ring, 4Å
Val	CB, 5Å
Cx in Fx	C1-C10, 4Å

To determine the Boltzmann-weighted ensemble of peptide conformations, the Daura clustering algorithm,[15]with a 2.5 Å cutoff for the RMDS in atomic positions for the entire bioconjugate backbone (the peptide backbone and all heavy atoms on the fatty acid chain) was employed. A similar analysis was conducted just for the peptide backbone only (neglecting the fatty acid chain), using a cutoff of 2.0 Å. These cutoffs have been established from previous work and are used here to enable compatibility in comparing with past studies. The clustering analysis was performed over the full 20,001 frames of the reference (λ=0.0) trajectory. The percentage population of each distinct structure was determined from the fraction of the total 20,001 frames that were assigned to that distinct structure.

The discrete conformational entropy based on the cluster analysis is defined as

$$S_{conf} = -\sum_{i=1}^{N_c} p_i \log(p_i)$$

where p_i is the fractional population (between 0 and 1) of the i^{th} cluster, and N_c is the total number of clusters.

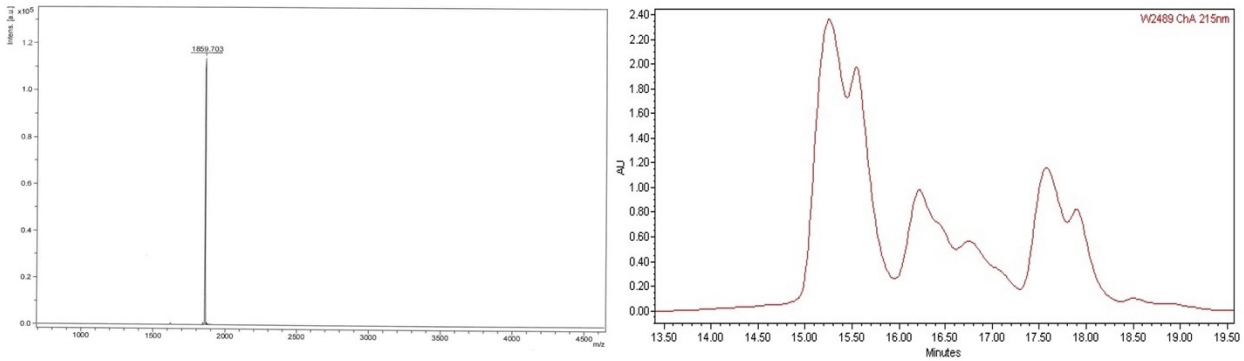

Figure S1. MALDI-TOF Mass Spectroscopy analysis (left) and chromatogram of HPLC (right) for P1CF$_6$.

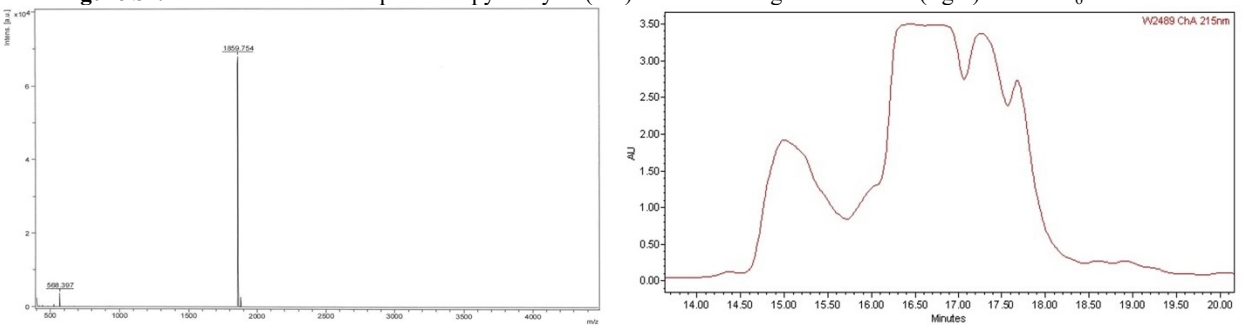

Figure S2. MALDI-TOF Mass Spectroscopy analysis (left) and chromatogram of HPLC (right) for F$_6$CP1.

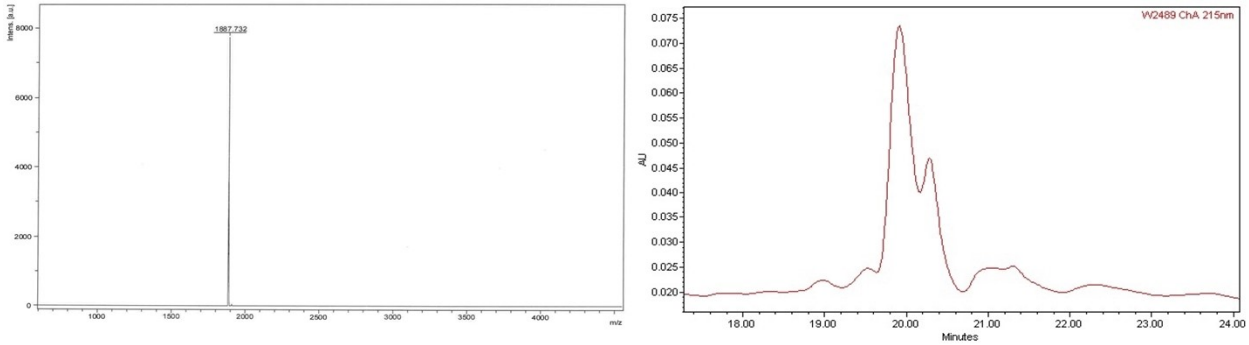

Figure S3. MALDI-TOF Mass Spectroscopy analysis (left) and chromatogram of HPLC (right) for P1CF$_8$.

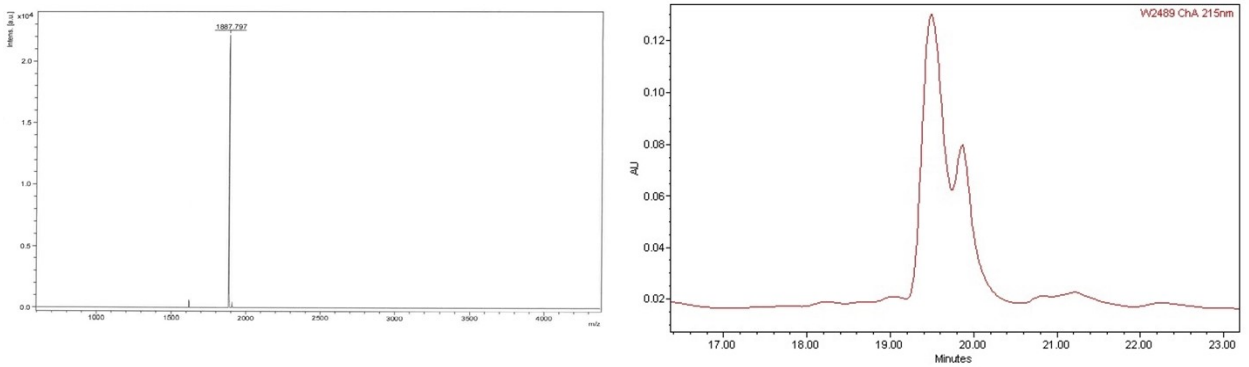

Figure S4. MALDI-TOF Mass Spectroscopy analysis (left) and chromatogram of HPLC (right) for F$_8$CP1.

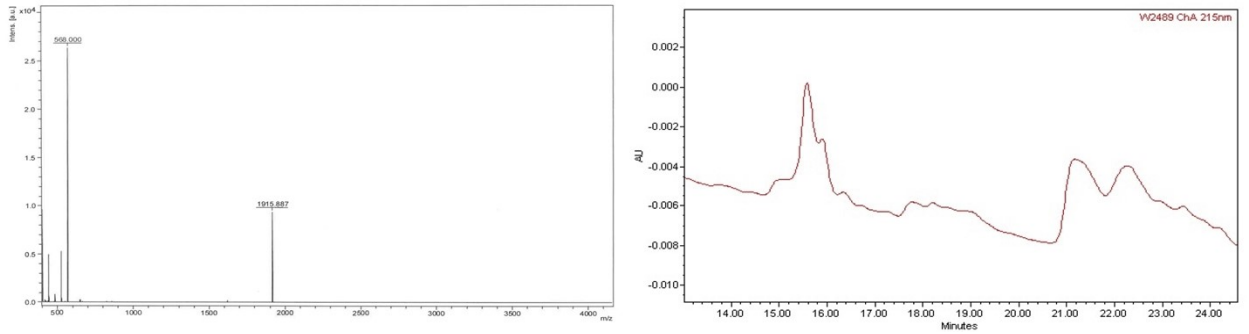

Figure S5. MALDI-TOF Mass Spectroscopy analysis (left) and chromatogram of HPLC (right) for $P1CF_{10}$.

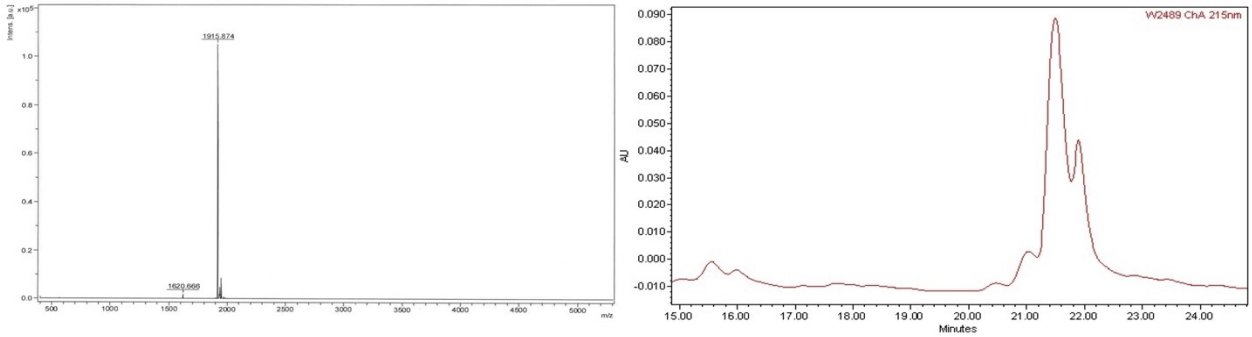

Figure S6. MALDI-TOF Mass Spectroscopy analysis (left) and chromatogram of HPLC (right) for $F_{10}CP1$.

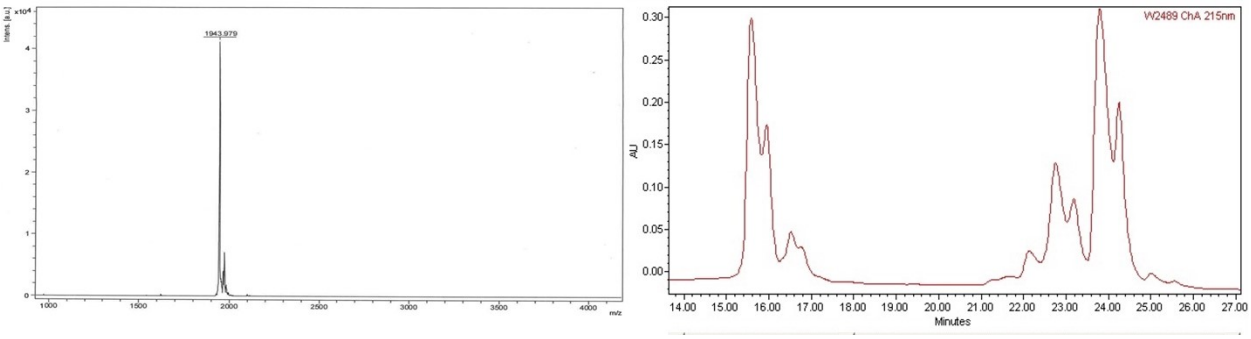

Figure S7. MALDI-TOF Mass Spectroscopy analysis (left) and chromatogram of HPLC (right) for $P1CF_{12}$.

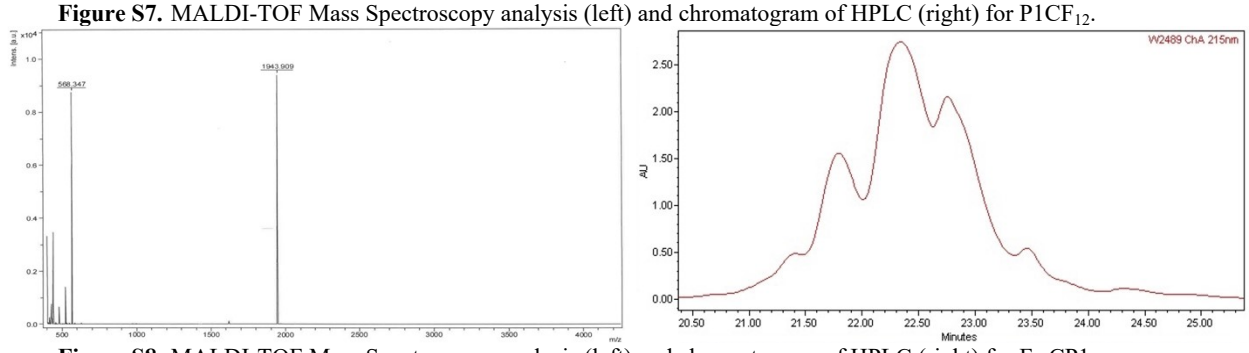

Figure S8. MALDI-TOF Mass Spectroscopy analysis (left) and chromatogram of HPLC (right) for $F_{12}CP1$.

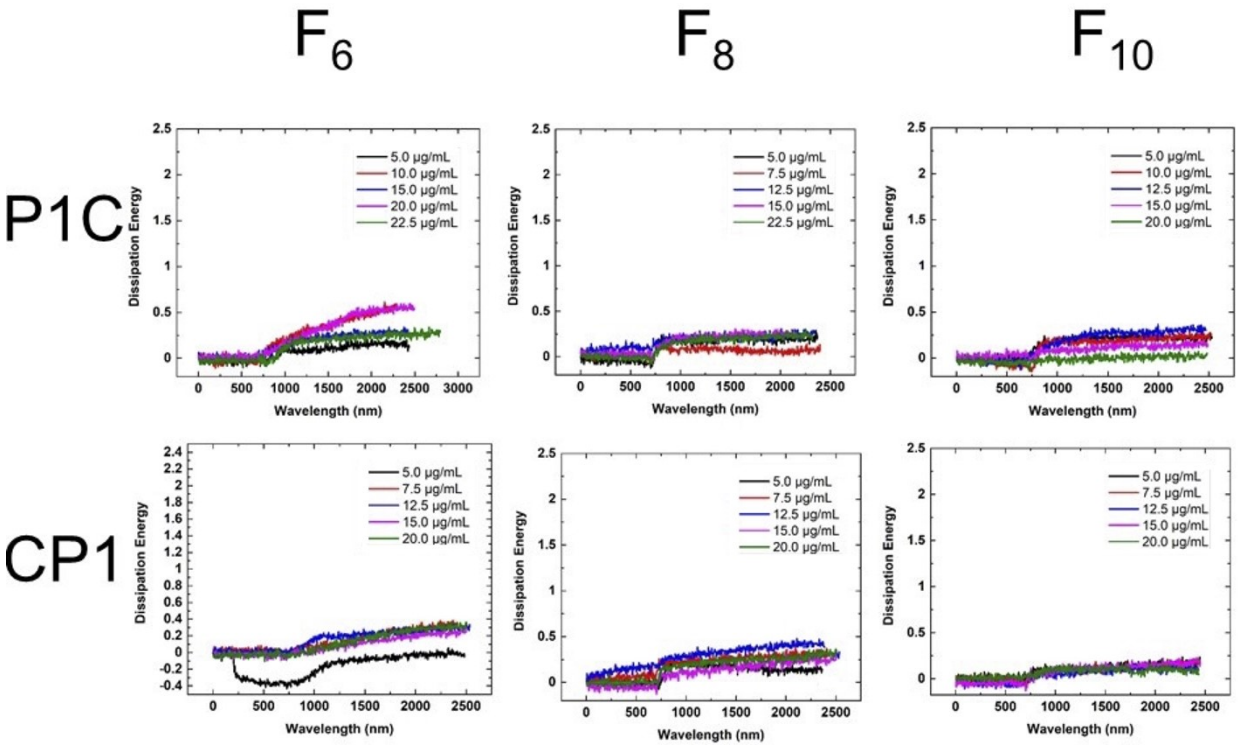

Figure S9. Dissipation energy of fatty-acid modified peptides for chain length 6-10 at N- and C-termini.

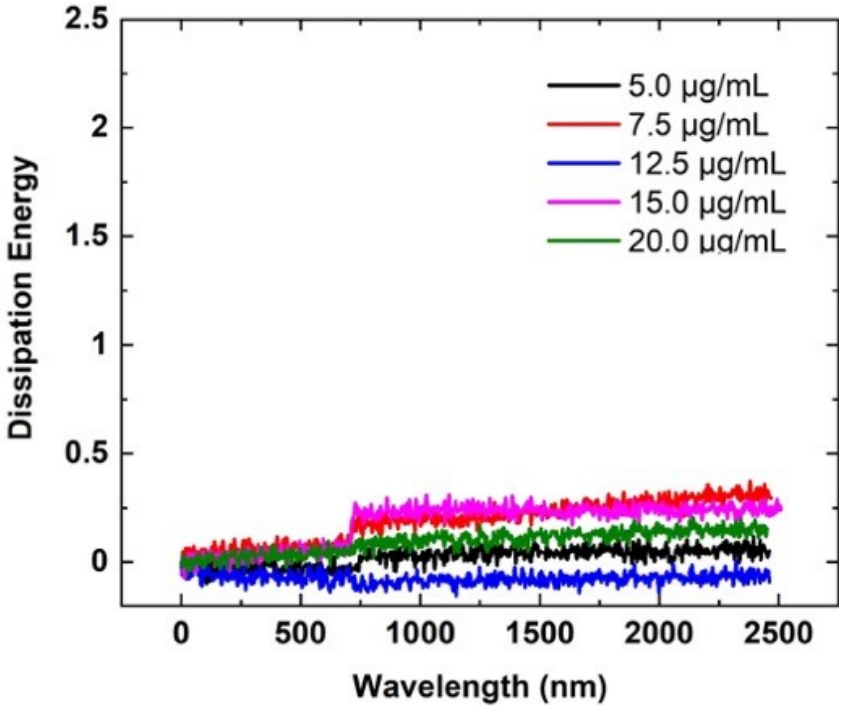

Figure S10. Dissipation energy over a range of concentrations for the parent peptide (P1).

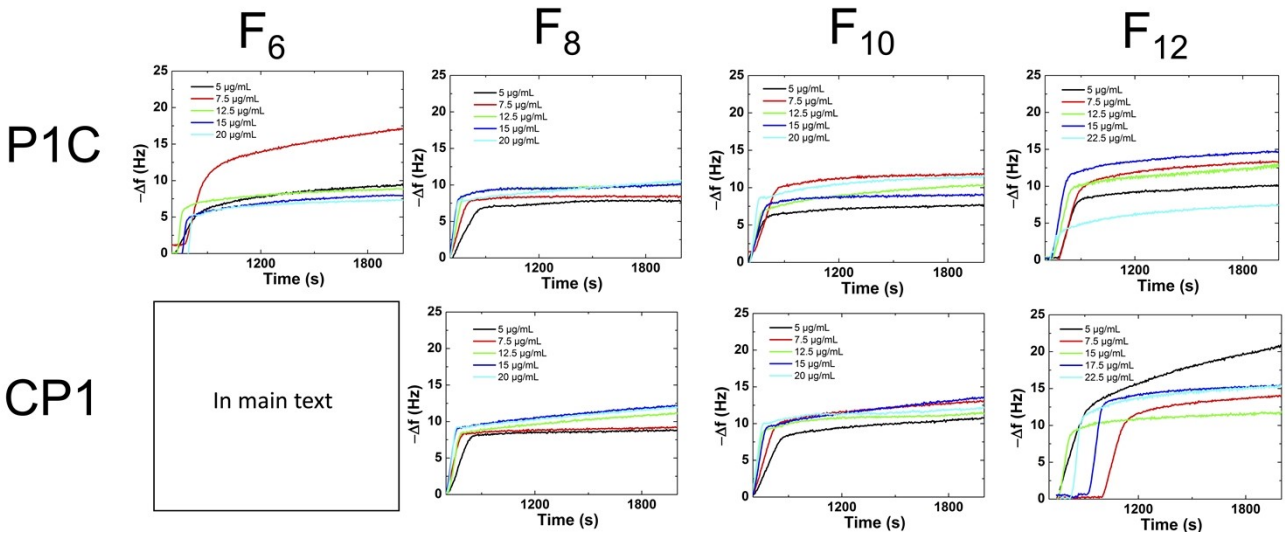

Figure S11. Sensogram of fatty-acid modified peptides for chain length 6-10 at N- and C-termini.

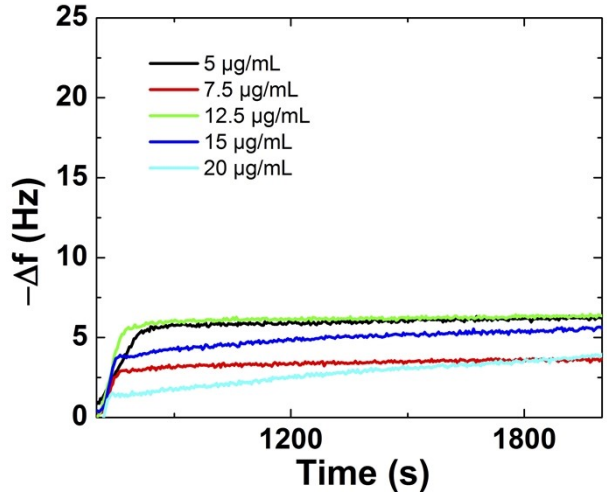

Figure S12. Sensogram for parent peptide (P1).

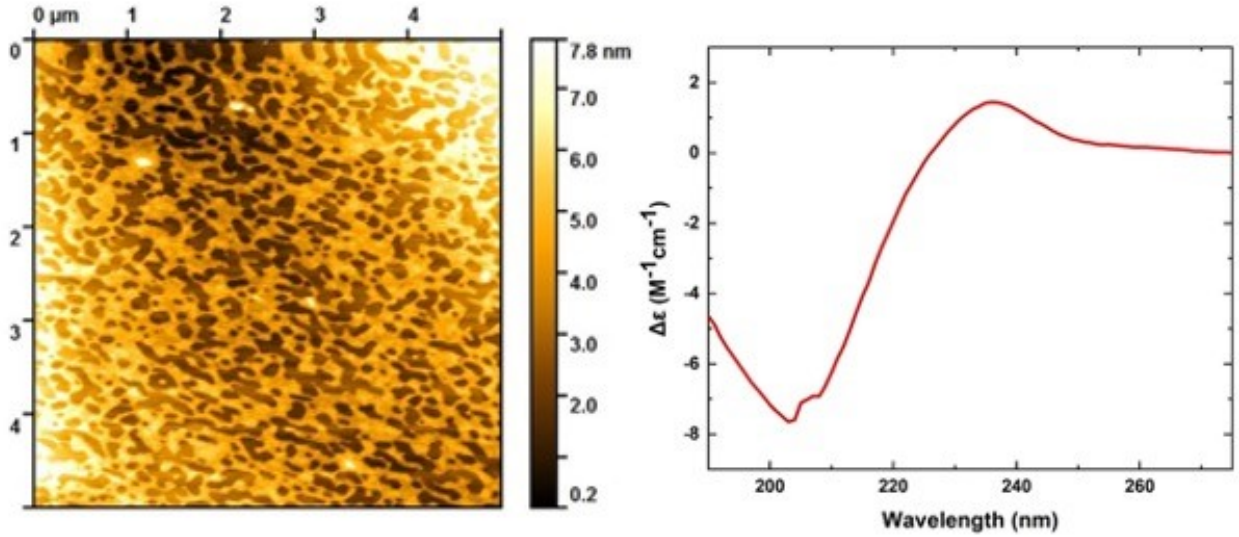

Figure S13. The AFM image of P1 on HOPG (left) and CD of P1 peptide in aqueous solution (right).

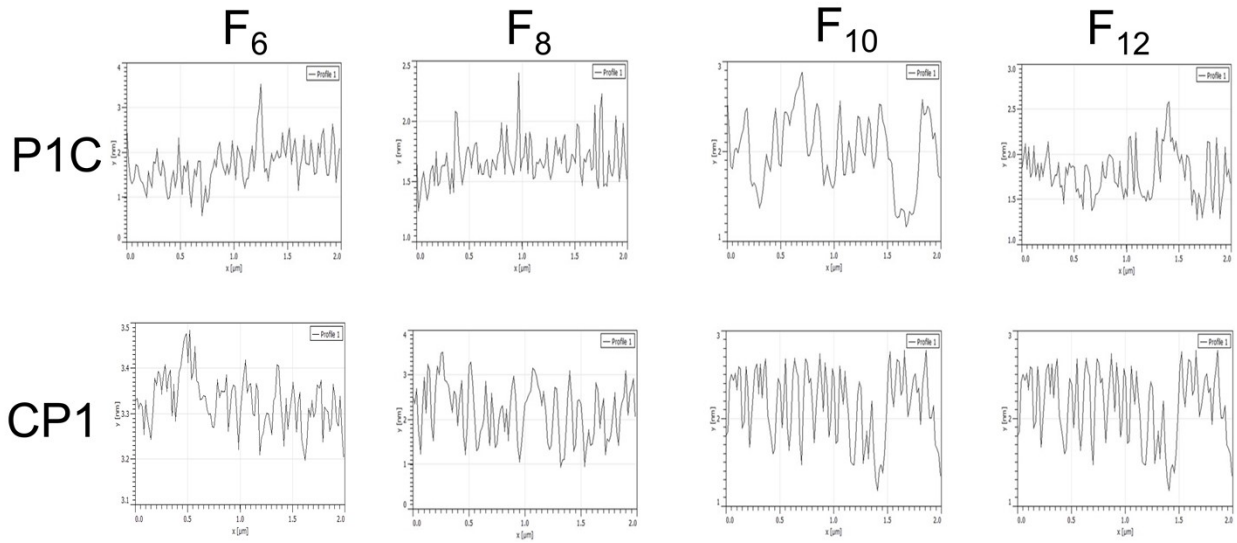

Figure S14. Height profile extracted from AFM images for each peptide on HOPG.

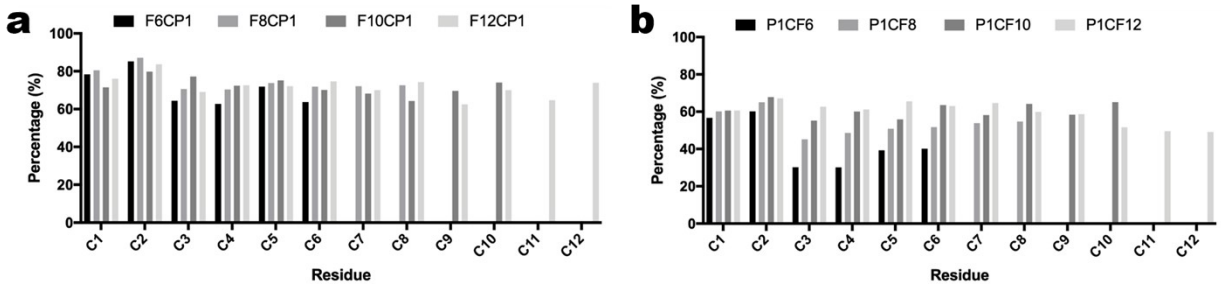

Figure S15. Full breakdown of residue-surface binding (expressed as a percentage of the total number of frames) for each site in the fatty-acid tail of the bioconjugates. a) F_nCP1, b) $P1CF_n$.

Table S2. Summary of the predicted enthalpic binding score (kJ mol^{-1}) expressed as the total score and partition into contributions from the peptide (labelled P1) and the fatty acid (labelled Fn, n=6,8,10,12) domains.

Binding scores (kJ/mol)				
F6CP1	-119.1	<	P1CF6	-115.9
F6	-44.3	<	F6	-26.7
P1	-64.9	>	P1	-81.2
F8CP1	-137.3	<	P1CF8	-126.8
F8	-62.3	<	F8	-44.7
P1	-64.5	>	P1	-73.5
F10CP1	-145.8	≃	P1CF10	-147.5
F10	-75.1	<	F10	-63.4
P1	-60.4	>	P1	-75.5
F12CP1	-162.2	≃	P1CF12	-158.1
F12	-89.8	<	F12	-74.2
P1	-62.1	>	P1	-74.5

Table S3. S_{conf} values (dimensionless) calculated for each of the bioconjugates considered in this study.

Sconf			
F6CP1	2.852	P1CF6	2.362
F8CP1	2.38	P1CF8	2.32
F10CP1	2.531	P1CF10	2.704
F12CP1	2.917	P1CF12	2.869

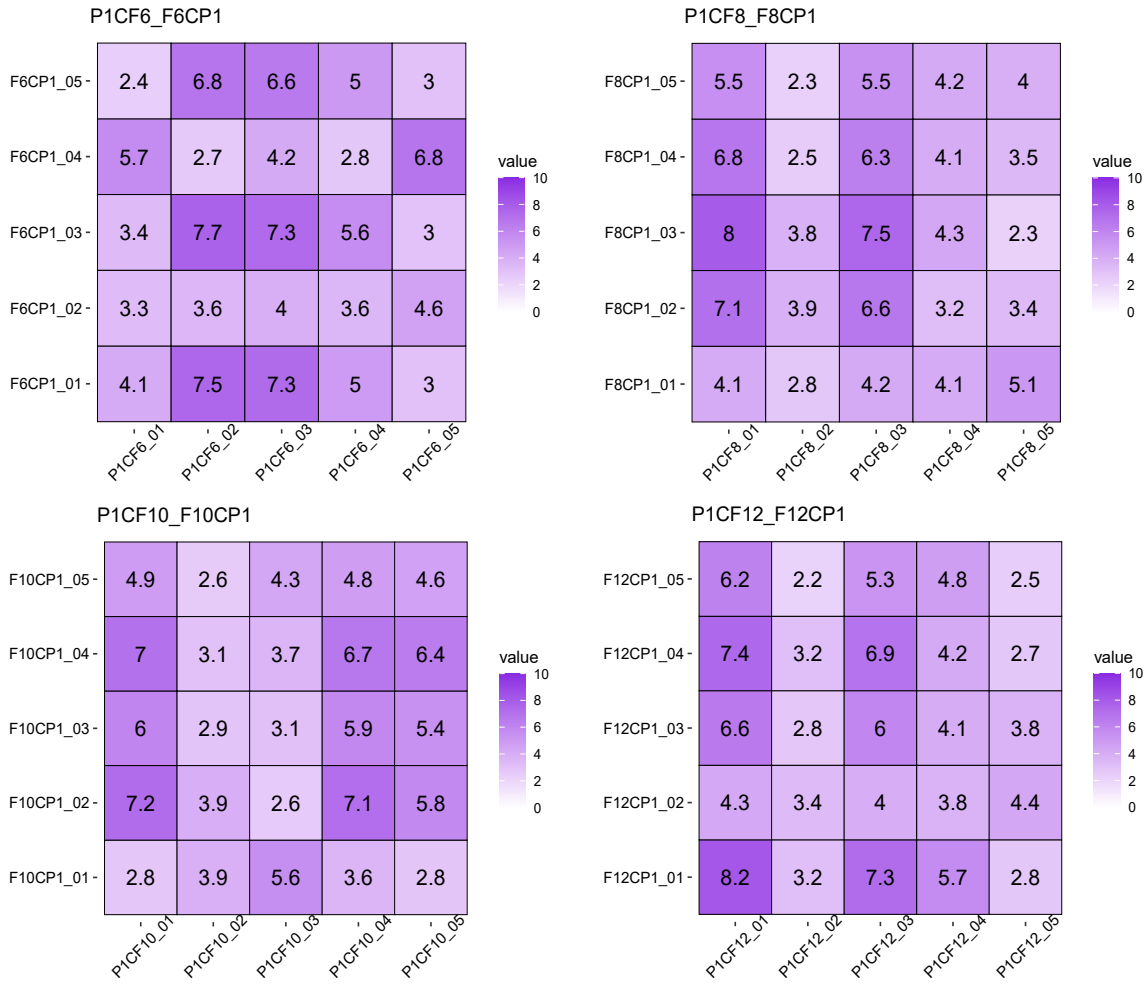

Figure S16. Cross-cluster analysis based on clustering of the P1 backbone atomic positions within the bioconjugate molecules. Comparison of peptide structural similarities for the top five most likely structures, based on root mean squared deviation of backbone atom positions (in units of Å). Values of 2.0 Å or less indicate a match.

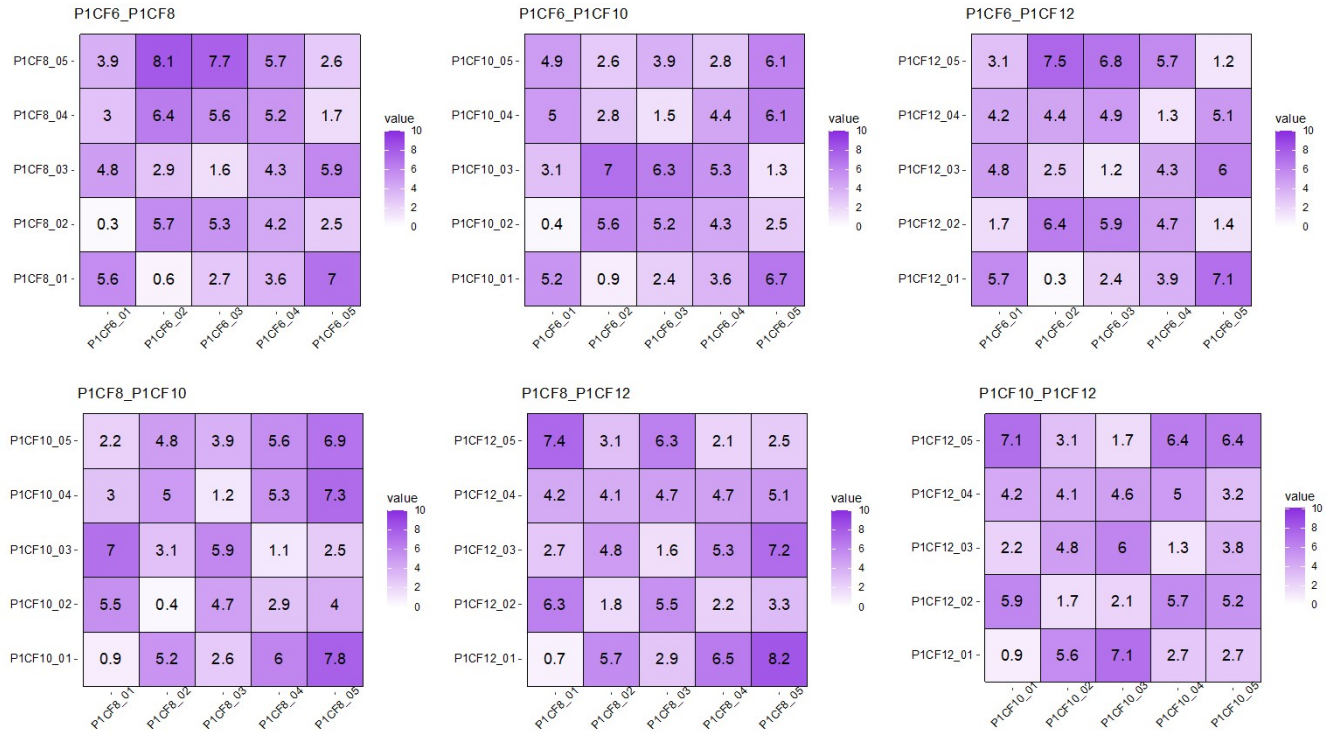

Figure S17. Cross-cluster analysis based on clustering of the P1 backbone atomic positions within the bioconjugate molecules. Comparison of peptide structural similarities for the top five most likely structures, based on root mean squared deviation of backbone atom positions (in units of Å). Values of 2.0 Å or less indicate a match.

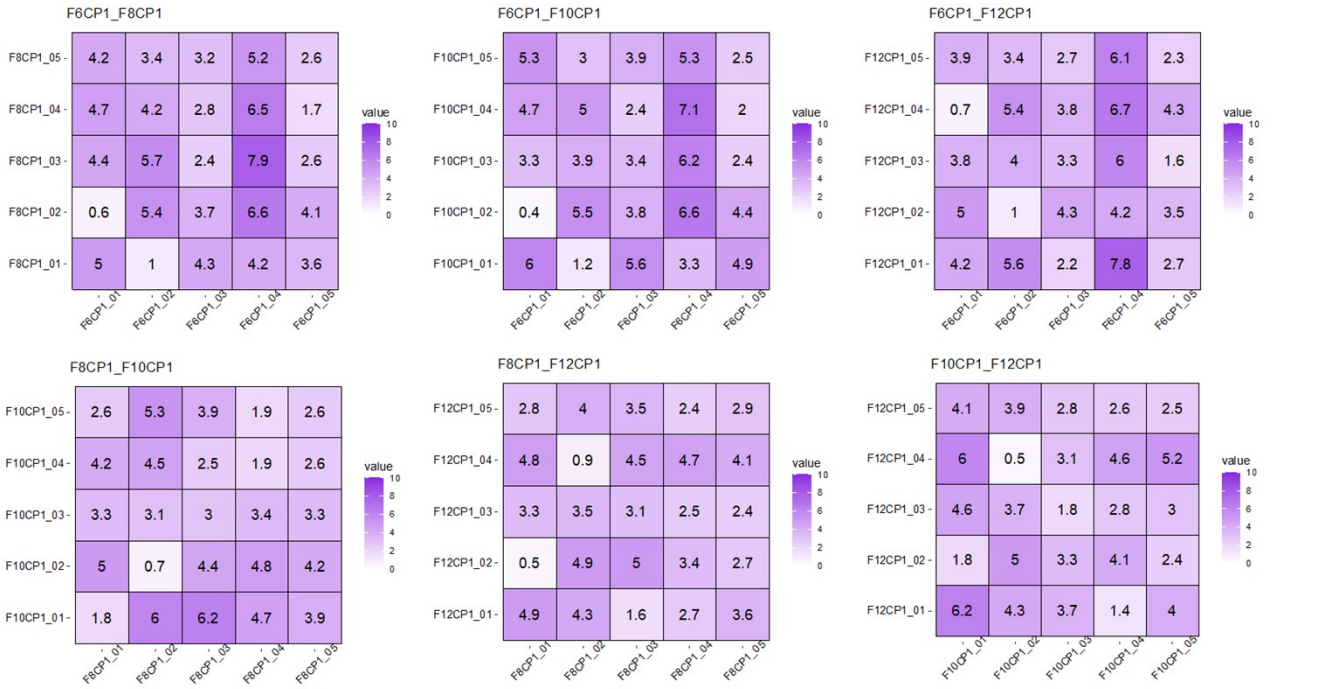

Figure S18. Cross-cluster analysis based on clustering of the P1 backbone atomic positions within the bioconjugate molecules, comparing different chain lengths but keeping the attachment point fixed (N-terminal). Comparison of peptide structural similarities for the top five most likely structures, based on root mean squared deviation of backbone atom positions (in units of Å). Values of 2.0 Å or less indicate a match,

References

1. T. Terakawa, T. Kameda, S. Takada, *J of Comput. Chem.* 2011, **32,** 1228-1234.
2. L. B. Wright, T. R. Walsh, *Phys. Chem. Chem. Phys.* 2013, **15**, 4715-4726.
3. M. J. Abraham, T. Murtola, R. Schulz, S. Páll, J. C. Smith, *SoftwareX* 2015, **1-2**, 19-25.
4. S. Nosé, *Mol. Phys.* 1984, **52**, 255-268.
5. W. G. Hoover, Phys Rev A Gen Phys 1985, **31**, 1695-1697.
6. T. Darden, D. York, L. Pedersen, *J. Chem. Phys.* 1993, **98,** 10089-10092.
7. A. D. MacKerell, D. Bashford, M. Bellott, R. L. Dunbrack, J. D. Evanseck, M. J. Field,; S. Fischer, J. Gao, H. Guo, S. Ha, D. Joseph-McCarthy, L. Kuchnir, K. Kuczera, F. T. K. Lau, C. Mattos, S. Michnick, T. Ngo, D. T. Nguyen, B. Prodhom, W. E. Reiher, B. Roux, M. Schlenkrich, J. C. Smith, R. Stote, J. Straub, M. Watanabe, J. Wiórkiewicz-Kuczera, D. Yin, M. Karplus, *J. Phys. Chem.* 1998, **18**, 3586-3616.
8. S. Piana, K. Lindorff-Larsen, D. E. Shaw, Biophys J 2011, **100**, L47-9.
9. J. P. Palafox-Hernandez, C.-K. Lim, Z. Tang, K. L. M. Drew, Z. E. Hughes, Y. Li, M. T. Swihart, P. N. Prasad, M. R. Knecht, T. R. Walsh, *ACS Appl. Mater. Interfaces*, 2016, **8**, 1050-1060.
10. Z. E. Hughes, S. M. Tomasio, T. R. Walsh, Nanoscale, 2014, 6, 5438-5448.
11. W. L. Jorgensen, J. Chandrasekhar, J. D. Madura, R. W. Impey, M. L. Klein, *Chem. Phys.* 1983, **79**, 926-935.
12. E. Neria, S. Fischer, M. Karplus, *Chem. Phys.* 1996, **105**, 1902-1921.
13. A. D. Parab, N. Bljak, M. R. Knecht, T. R. Walsh, *Adv. Mater. Interfaces*, 2021, **8,** 2001659.
14. Z. E. Hughes, T. R. Walsh, *J Mater Chem B,* 2015, **3**, 3211-3221.
15. X. G. K. Daura, B. Jaun, D. Seebach, W. F. van Gunsteren, A. E. Mark, *Angew. Chem. Int. Ed.* 1999, ***38*,** 236-240.